

Cyclic Naphthalene Diimide with a Ferrocene Moiety as a Redox-Active Tetraplex-DNA Ligand

著者	Kaneyoshi Shuma, Zou Tingting, Ozaki Shunsuke, Takeuchi Ryusuke, Udou Ayano, Nakahara Takumi, Fujimoto Kazuhisa, Fujii Satoshi, Sato Shinobu, Takenaka Shigeori
journal or publication title	Chemistry - A European Journal
volume	26
number	1
page range	139-142
year	2019-11-03
URL	http://hdl.handle.net/10228/00008205

doi: <https://doi.org/10.1002/chem.201903883>

Cyclic naphthalene diimide carrying ferrocene moiety as a redox-active tetraplex DNA ligand

Shuma Kaneyoshi^a, Tingting Zou^{a,b,*}, Shunsuke Ozaki^a, Ryusuke Takeuchi^a, Ayano Udou^a, Takumi Nakahara^a, Kazuhisa Fujimoto^c, Satoshi Fujii^d, Shinobu Sato^{a,b}, Shigeori Takenaka^{a,b,*}

Abstract: Cyclic naphthalene diimides (cNDI) carrying ferrocene moiety (cFNDs), **2–4** with different linker length between ferrocene and cNDI, were designed and synthesized as a redox-active tetraplex DNA ligand. Intramolecular stacking was observed between ferrocene and NDI planes of **2–4**, which could affect their binding property for G-quadruplex. Interestingly, the Circular Dichroism (CD) spectra of **2** clearly showed new cotton effects around 320–380 nm and 240 nm, which also can be considered as a direct evidence to prove the intramolecular stacking between ferrocene and NDI. When towards recognizing hybrid G-quadruplex, **3** and **4** showed 10^6 M⁻¹ order of binding affinity, while **2** was comparatively weaker, due to its more rigid structure. **2–4** also showed higher selectivity for G4 during electrochemical detection than non-cyclic FND derivatives, which further identified cFNDs' redox-active potentiality. cFND **2** and **3** even preferred to inhibit cancer cell growth than the normal cell in lower concentration range, suggesting the potentiality of cFNDs for bio-application.

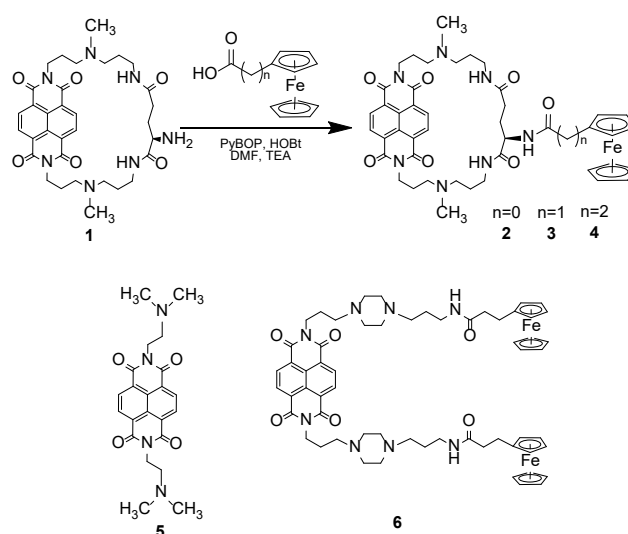
DNA carrying guanine (G)-rich sequence is known to form tetraplex DNA with folding through G-quartet structure, which is formed by four Gs with Hoogsteen hydrogen bonding^[1]. Due to the potential roles of G-quadruplex playing in telomere region and cancer-related genes promoter region, G4 ligand, which can stabilize tetraplex DNA structure, is expected to be a good candidate for an effective anti-cancer drug^[2]. Until now, huge series of tetraplex DNA specific ligands have been reported^[3]. As one group of G4 ligands, naphthalene diimide derivatives, containing electron-deficient aromatic ring, are expected to form stronger interaction with G-quartet carrying electron-rich four guanines, and result in a stable naphthalene diimide - tetraplex DNA complex^[4]. For better *in vivo* performance, it is also quite important to explore G4 ligands possessing higher preference for tetraplex DNA than duplex DNA, under the presence of excess amount of duplex DNA in genome^[3c]. As a successful candidate, naphthalene diimide carrying three substitutes showed high specificity for tetraplex DNA and potentiality for human pancreatic ductal adenocarcinoma therapy^[5]. Previously our group and Milelli group have reported cyclic naphthalene diimides (cNDI), which were constructed by connecting the two substituents of naphthalene diimide, they showed high affinity to selectively bind

to tetraplex DNA whereas almost no interaction with duplex DNA^[6]. Similar cyclic perylene diimide also was reported with much higher preference for tetraplex DNA^[7]. This may come from the steric hindrance of the linker chain of cNDI during the intercalation with duplex DNA or the stacking interaction for DNA bases.

On the other hand, ferrocene derivatives, which was commonly utilized as the signaling part of electrochemical biosensor^[8], also have been reported as an anti-cancer drug^[9]. Many ferrocenyl compounds display interesting cytotoxic, antitumor and DNA-cleaving activity. Therefore, the medicinal application of ferrocene is an active research area and many reports have shown that ferrocene derivatives have a promising activity *in vitro* and *in vivo* against several diseases^[10]. Although the mechanism of action is still rather unclear, it was proposed that oxidation of ferrocene to ferrocenium cation by redox enzymes leads to generation of reactive oxygen species (ROS), which in turn take part in DNA damage, resulting in cell death^[11].

In this study, as the first example, we conjugated G4 selective ligand cNDI with ferrocene, to generate a novel G-quadruplex targeting compound cFNDs. As shown in Scheme 1, cFND **2–4** were designed and synthesized with the condensation reaction of cyclic naphthalene diimide having amino moiety **1**^[12] with ferrocene-carboxylic acid, -acetic acid, and -propionic acid, respectively (synthesis details were list in supplementary information). They were expected with different redox potentials for their different length between ferrocene and linker amine part.

Their interactions with tetraplex DNA were investigated using spectrophotometric, isothermal titration calorimetric (ITC), and electrochemical techniques. Molar absorptivity values of **2–4** were calculated as 20,400 cm⁻¹ M⁻¹ at 387 nm, 23,200 cm⁻¹ M⁻¹ at 385 nm, and 21,600 cm⁻¹ M⁻¹ at 385 nm. These values were smaller



Scheme 1. Synthesis of cyclic naphthalene diimides carrying ferrocene moiety, **2–4**, from precursor **1** and non-cyclic naphthalene diimides **5** and **6**.

[a] S. Kaneyoshi, Dr. T. Zou, S. Ozaki, R. Takeuchi, A. Udou, Dr. S. Sato, Prof. S. Takenaka, Department of Applied Chemistry, Kyushu Institute of Technology, Fukuoka, 804-8550, Japan.

[b] Dr. T. Zou, Dr. S. Sato, Prof. S. Takenaka, Research Center for Bio-microsensing Technology, Kyushu Institute of Technology, Fukuoka, 804-8550, Japan.

[c] Dr. K. Fujimoto, Department of Applied Chemistry and Biochemistry, Kyushu Sangyo University, Fukuoka 813-8503, Japan.

[d] Dr. S. Fujii, Department of Bioscience and Bioinformatics, Kyushu Institute of Technology, Fukuoka 820-8502, Japan

[*] Corresponding author
shige@che.kyutech.ac.jp; zoutt@che.kyutech.ac.jp

COMMUNICATION

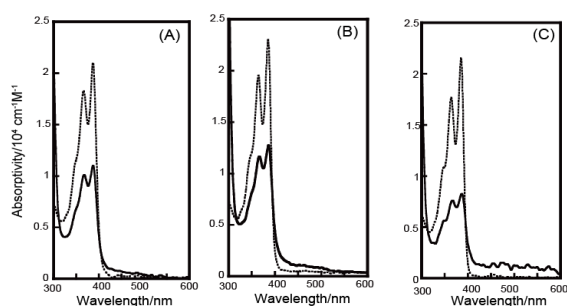


Figure 1. Absorption spectra of 8.1 μM cFND **2** (A), 6.1 μM **3** (B), or 8.1 μM **4** (C) in the absence (dashed line) or presence (solid line) of 13 μM *Telomere G1*. Buffer: 100 mM AcOK-AcOH (pH5.5) and 100 mM KCl.

than naphthalene diimide derivative **5** of 26,600 $\text{cm}^{-1}\text{M}^{-1}$ reported previously^[13]. The order of hypochromic effect is $2 < 4 < 3$ (23%, 13%, and 19%, respectively), which suggested that these hypochromic effects seems to be correlated with the efficiency of the intramolecular stacking between the planes of ferrocene and naphthalene diimide rings. Shortest **2** possibly has most effective intramolecular staking space, and longest **4** has enough length and flexibility for intramolecular stacking, while intermediate length of **3** may impair its flexibility for effective stacking. Besides, **2** showed the maximum absorption with around 2nm of red shift comparing to that of **3** and **4**, which also indicated the highest intramolecular stacking ability.

Hybrid G-quadruplex sequence (Human telomere DNA sequence, *Telomere G1*: 5'-TAG GGT TAG GGT TAG GGT TAG GG-3') and parallel G-quadruplex sequence (*c-myc*: 5'-TGA GGG TGG GGA GGG TGG GGA A-3') were utilized as G-quadruplex model^[12] for investigating their interaction with **2-4**. Absorption spectra of 8.1 μM cFND **2**, 6.1 μM **3**, or 8.1 μM **4** were measured in the absence or presence of 13 μM *Telomere G1* as shown in Fig. 1. Upon addition of *Telomere G1*, obvious hypochromic effects of 46%, 50%, or 59% were observed in the case of **2-4**, respectively (Fig. 1). These results indicated that the naphthalene diimide ring of **2-4** could bind to G-quartet planes.

ITC was adopted to analyze binding affinity (K_a) of **2-4** to single tetraplex DNA, the obtained binding parameters were summarized in Table 1 and Figure S13-14. Naphthalene diimide generally bound to G-quartet interface with extensive π - π contacts^[4], and cFND **2-4** bound to tetraplex DNA with $n=2$, which suggested that two molecules of cFNDs bound to G-quartets from top and bottom sites. Binding ratio commonly could be obtained through binding kinetic measurements such as SPR^[14] and UV-Vis^[15], previously 2:1 ligand/quadruplex complex (MK2L2) also have been reported by ESI-MS^[16], here ITC we adopted could also provide the information for investigating the possible binding chiometry of ligand and G-quadruplex. According to the

thermodynamic parameters during the interaction of **2-4** with *Telomere G1* and *c-myc* shown in Table 1, positive ΔS values were obtained for all **2-4**, which indicated that linking ferrocene to cyclic naphthalene diimide did not unfavour the binding of naphthalene diimide for G-quartet. For parallel G-quadruplex (*c-myc*), **2-4** all showed similar binding affinity around 10^6 M^{-1} order (**2** was slightly weaker). However, for hybrid G-quadruplex (*Telomere G1*), although **3** and **4** still showed 10^6 M^{-1} order binding affinity, whereas **2** was only in 10^5 M^{-1} order (almost 10 times weaker than **3** and **4**). Regarding the structure, *Telomere G1* hybrid G-quadruplex contains a big loop part^[17], which may interfere its G-quartet interacting with rigid **2**, while, **3** and **4** might be able to make some shift during the interaction benefiting from the longer length.

CD spectra were further analyzed to identify the recognition of **2-4** for G-quadruplex. Figure 2 and Figure S15 showed the CD spectra of 1.5 μM *Telomere G1* or *c-myc* upon addition of **2, 3**, or **4**. Typical pattern of parallel G-quadruplex (*c-myc*) and hybrid G-quadruplex (*Telomere G1*) CD spectra were confirmed. For *c-myc*, after adding **2-4**, CD spectra intensities of positive cotton effect decreased, but the spectra shapes were still the same, which suggested cFNDs binding did not impair the parallel G-quadruplex. For *Telomere G1*, after adding **3-4**, similar phenomenon could be observed as for *c-myc*. However, after adding **2**, significant negative cotton effect around 240 nm and 320-380 nm were obtained, and this behavior was finally identified that originated from **2** (Figure S15). Although three different cFNDs were prepared, only **2** exhibited obvious CD spectra (Figure 2C). This might be attributed to that **2** has the shortest linker, which restricted the flexibility of ferrocene, in turn enhanced the intramolecular stacking between ferrocene and NDI, and helped **2** form a rigid structure with chirality and triggered the strong cotton effect of ferrocene around 240 nm.

Melting temperature of 1.5 μM *Telomere G1* was monitored by CD spectra at 288 nm in the absence or presence of 4.5 μM **2-4** to obtain the melting curve. Figure 2D and Figure S16 showed the ΔT_m for **2, 3**, or **4** were 2.0, 3.3, or 5.0 $^{\circ}\text{C}$, respectively. **2-Telomere G1** complex showed the weakest stability. During performing the simulation modeling of cFNDs with G-quadruplex, ferrocene of **3** and **4** showed better flexibility during binding, while ferrocene of **2** was almost unadjustable, and **2** binding to *Telomere G1* might cause some conformational strain (Figure 2E).

The redox activity of **2-4** were analyzed with adopting the 6-MH (to avoid non-specific adsorption) or tetraplex DNA immobilized gold electrodes. Cyclic voltammograms of 20 μM **2-4** was measured at room temperature as shown in Figure S17 and electrochemical parameters were summarized in Table S1. The $E_{1/2S}$ value representing the redox potentials was $2 > 3 > 4$, which was in accordant with the order of electro density of ferrocene

Table 1. ITC-derived thermodynamic parameters for the interactions of cFNDs **2-4** with *Telomere G1* and *c-myc* at 30 $^{\circ}\text{C}$.

	<i>Telomere G1</i>			<i>c-myc</i>		
	2	3	4	2	3	4
n	2	2	2	2	2	2
$K_a / 10^5 \text{ M}^{-1}$	1.5 \pm 0.2	12.6 \pm 7.6	11.4 \pm 1.0	8.7 \pm 2.5	12.0 \pm 0.3	18.4 \pm 1.0
$\Delta H^{\circ} / \text{kcal mol}^{-1}$	-3.2 \pm 0.2	-3.2 \pm 0.1	-4.0 \pm 0.1	-3.9 \pm 0.2	-3.7 \pm 0.0	-3.4 \pm 0.1
$T\Delta S^{\circ} / \text{kcal mol}^{-1}$	4.0 \pm 0.3	5.3 \pm 0.1	4.4 \pm 0.0	4.4 \pm 0.3	4.8 \pm 0.0	5.3 \pm 0.1
$\Delta G^{\circ} / \text{kcal mol}^{-1}$	-7.2 \pm 0.8	-8.5 \pm 0.0	-8.4 \pm 0.1	-8.2 \pm 0.2	-8.4 \pm 0.0	-8.7 \pm 0.0

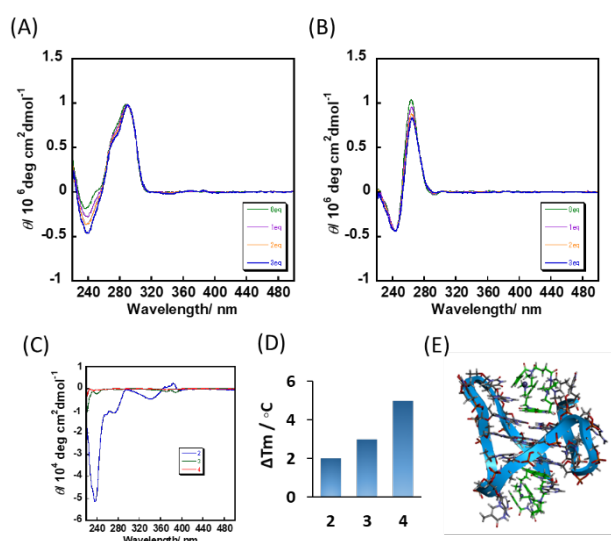


Figure 2. CD spectra of 1.5 μM *Telomere G1* (A) or *c-myc* (B) upon addition of **2**. Buffer: 100 mM AcOK-AcOH (pH5.5) and 100 mM KCl at 25 $^{\circ}\text{C}$. Ligand vs. DNA; 0:1 (Green); 1:1 (Purple); 2:1 (Orange); 3:1 (Blue); (C) CD spectra of **2-4**; (D) ΔT_m of *Telomere G1* with adding **2**, **3** and **4**; (E) Molecular modelling of **2** with hybrid telomere G-quadruplex. PDB: 2gku.

(carbonyl moiety attached to ferrocene ring led to decreasing electron density and resulted in the highest positively sifted redox potential). The current intensities of **2-4** (i_{pa}) were higher in tetraplex DNA immobilized electrode than that in the electrode immobilized by 6-MH. These results suggested that **2-4** could be concentrated with tetraplex DNA on the electrode and still displayed redox activity. Besides, when comparing to non-cyclic FND-**6**, **2-4** showed higher selectivity for G-quadruplex than single strand DNA according to CC and SWV technique^[19] (2-2.7 folds higher than **6**), which suggested a better potential of **2-4** for electrochemical detection (Table S2).

Furthermore, to investigate the potential of cFNDs for bio-application, two cell lines, *Hela* (cancer cell line) and *ASF-4-4L2* (Normal diploid fibroblast) were adopted to conduct the cell growth inhibition activity with treating **2-4**. A 48 h (2 days) exposure with different concentrations (ranging from 0.01 to 10 μM) of cFNDs resulted in a remarkable and concentration-dependent inhibition of cell growth. IC_{50} and IC_{25} (concentrations of compounds leading 50% and 25% inhibition of cell proliferation) were calculated in non-linear regression analysis mode. When comparing the IC_{50} of cFNDs for *Hela* and *ASF-4-4L2*, general similar values were obtained and no significant preference for selectively inhibiting cancer cell growth could be observed (Table 2, Figure S18). However, the IC_{50} were around 3 μM , which was comparable to some previous reported naphthalene diimide or ferrocene derivatives^[11a, 18]. Besides, **2** and **3** showed much lower

Table 2. Cell growth inhibition assay of **2-4** for cancer cell line *Hela* and normal fibroblast cell line *ASF-4-4L2*.

	IC_{50} (μM)		IC_{25} (μM)	
	<i>Hela</i>	<i>ASF-4-4L2</i>	<i>Hela</i>	<i>ASF-4-4L2</i>
2	2.3 \pm 0.6	3.9 \pm 0.3	0.2 \pm 0.1	2.7 \pm 0.3
3	3.2 \pm 0.6	2.8 \pm 0.2	0.8 \pm 0.3	2.0 \pm 0.2
4	2.9 \pm 0.6	1.9 \pm 0.1	0.8 \pm 0.3	1.2 \pm 0.1

IC_{25} value for *Hela* cell than *ASF-4-4L2*. When treating cFND-**2** with 2.5 μM , *ASF-4-4L2* were still alive for around 76%, while *Hela* cell only showed 46% viability (IC_{25} was 0.2 μM for *Hela*, and 2.7 μM for *ASF-4-4L2*), which indicated that, **2** and **3** might be potential for bio-applications under optimized concentration.

In conclusion, here we reported a new group of conjugators, cyclic naphthalene diimide and ferrocene (cFND **2-4**) as redox-active tetraplex DNA ligand. **2** with the shortest linker between ferrocene and NDI displayed the most obvious intramolecular stacking and triggered chemical-derived new cotton effect. **2-4** showed the ability to recognize and stabilize G-quadruplex, and also better potentiality for electrochemical detection than non-cyclic FND. **2** and **3** also displayed lower cytotoxicity for normal cell than cancer cell in low concentration range.

Experimental Section

Experimental Details were described in the supporting information file.

Acknowledgements

This study was supported in part by the Nakatani Foundation for advancement of measuring technologies in biomedical engineering, Japan (S.T.) and by Grants-in-Aid from the Ministry of Education, Culture, Sports, Science, and Technology, Japan (19H02748, S.T.).

Keywords: G-quadruplex, ferrocene, cyclic naphthalene diimide, electrochemistry, anti-tumor, chirality

- [1] H. J. Lipps, D. Rhodes, *Trends Cell Biol* 2009, 19, 414-422.
- [2] a) J. H. Tan, L. Q. Gu, J. Y. Wu, *Mini Rev Med Chem*. 2008, 8, 1163-1178; b) G. Cimino-Reale, N. Zaffaroni, M. Folini, *Curr Pharm Des*. 2016, 22, 6612-6624.
- [3] a) S. Asamitsu, T. Bando, H. Sugiyama, *Chem. Eur. J.* 2019, 25, 417-430; b) A. R. Duarte, E. Cadoni, A. S. Ressurreicao, R. Moreira, A. Paulo, *ChemMedChem* 2018, 13, 869-893; c) M. Zuffo, A. Guedin, E. D. Leriche, F. Doria, V. Pirota, V. Gabelica, J. L. Mergny, M. Freccero, *Nucleic Acids Res.* 2018, 46, e115; d) V. Pirota, M. Nadai, F. Doria, S. N. Richter, *Molecules* 2019, 24.
- [4] G. W. Collie, R. Promontorio, S. M. Hampel, M. Micco, S. Neidle, G. N. Parkinson, *J Am Chem Soc* 2012, 134, 2723-2731.
- [5] a) M. Micco, G. W. Collie, A. G. Dale, S. A. Ohnmacht, I. Pazitna, M. Gunaratnam, A. P. Reszka, S. Neidle, *J. Med. Chem.* 2013, 56, 2959-2974; b) S. M. Hampel, A. Sidibe, M. Gunaratnam, J. F. Riou, S. Neidle, *Bioorg. Med. Chem. Lett.* 2010, 20, 6459-6463.
- [6] a) Y. Esaki, M. M. Islam, S. Fujii, S. Sato, S. Takenaka, *Chem. Commun. (Camb)* 2014, 50, 5967-5969; b) C. Marchetti, A. Minarini, V. Tumiatti, F. Moraca, L. Parrotta, S. Alcaro, R. Rigo, C. Sissi, M. Gunaratnam, S. A. Ohnmacht, S. Neidle, A. Milelli, *Bioorg. Med. Chem.* 2015, 23, 3819-3830.
- [7] S. Vasimalla, S. Sato, F. Takenaka, Y. Kurose, S. Takenaka, *Bioorg Med Chem* 2017, 25, 6404-6411.
- [8] Shigeori Takenaka, Kenichi Yamashita, Makoto Takagi, Yoshihiro Uto, and Hiroki Kondo, *Anal. Chem.* 2000, 72, 1334-1341.
- [9] a) D. R. van Staveren, N. Metzler-Nolte, *Chem. Rev.* 2004, 104, 5931-5985; b) B. Lal, A. Badshah, A. A. Altaf, M. N. Tahir, S. Ullah, F. Huq, *Dalton Trans.* 2012, 41, 14643-14650.
- [10] M. F. R. Fouda, M. M. Abd-Elzaher, R. A. Abdelsamaia, A. A. Labib, *Applied Organometallic Chemistry* 2007, 21, 613-625.
- [11] a) M. Bartosik, L. Koubkova, J. Karban, L. Cervenkova Stastna, T. Hodik, M. Lamac, J. Pinkas, R. Hrstka, *Analyst* 2015, 140, 5864-5867. b)

COMMUNICATION

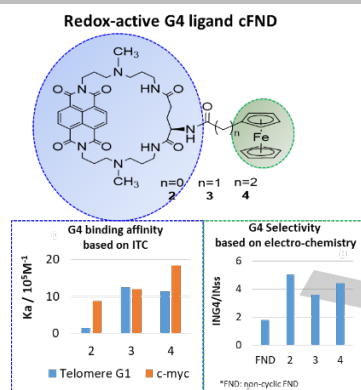
- Domenico Osella, Marco Ferrali, Marco Fontani, Carlo Nervi, P. Z., Franco Laschi, Giorgio Cavigliolo, *Inorganica Chimica Acta* 2000, 306, 42-48.
- [12] R. Takeuchi, T. Zou, D. Wakahara, Y. Nakano, S. Sato, S. Takenaka, *Chemistry* 2019, 25, 8691-8695.
- [13] F. A. Tanius, S. F. Yen, W. D. Wilson, *Biochemistry* 1991, 30, 1813-1819.
- [14] S. Asamitsu, Y. Li, T. Bando, H. Sugiyama, *ChemBiochem* 2016, 17, 1317-1322.
- [15] M. M. Islam, S. Fujii, S. Sato, T. Okauchi, S. Takenaka, *Molecules* 2015, 20, 10963-10979.
- [16] A. Marchand, F. Rosu, R. Zenobi, V. Gabelica, *J Am Chem Soc* 2018, 140, 12553-12565.
- [17] K. N. Luu, A. T. Phan, V. Kuryavyi, L. Lacroix, D. J. Patel, *J Am Chem Soc* 2006, 128, 9963-9970.
- [18] a) A. Pasini, C. Marchetti, C. Sissi, M. Cortesi, E. Giordano, A. Minarini, A. Milelli, *ACS Med. Chem. Lett.* 2017, 8, 1218-1223; b) M. Arevalo-Ruiz, F. Doria, E. Belmonte-Reche, A. De Rache, J. Campos-Salinas, R. Lucas, E. Falomir, M. Carda, J. M. Perez-Victoria, J. L. Mergny, M. Freccero, J. C. Morales, *Chem. Eur. J.* 2017, 23, 2157-2164.
- [19] S. Sato, A. Kajima, H. Hamanaka, S. Takenaka, *J. Organomet. Chem.* 2019, 897, 107-113.

Entry for the Table of Contents

Layout 1:

COMMUNICATION

Cyclic naphthalene diimides carrying ferrocene moiety (cFNDs), were designed and synthesized as a redox-active tetraplex DNA selective ligand. These cFNDs showed comparatively high binding affinity for G-quadruplex, and also higher selectivity for G-quadruplex when applying for electrochemical detection.



Shuma Kaneyoshi^a, Tingting Zou^{a,b,*},
Shunsuke Ozaki^a, Ryusuke Takeuchi^a,
Ayano Udou^a, Takumi Nakahara^a,
Kazuhisa Fujimoto^c, Satoshi Fujii^d,
Shinobu Sato^{a,b}, Shigeori Takenaka^{a,b,*}

Page No. – Page No.

Cyclic naphthalene diimide carrying ferrocene moiety as a redox-active tetraplex DNA ligand